

Imager to Spectrometer: Extracting Spectral Data from the Two-dimensional Array

Richard J. Nelson*

Solid State Scientific Corporation
27-2 Wright Road, Hollis, New Hampshire 03049

ABSTRACT

A common technique in the design of a spectral imaging system is the use of a prism as the dispersive element to disperse the colors onto the focal plane. The imaging system can serve as a spectrometer for point events with minimal computational load because the spectral data from a point event is spread directly on the FPA. The fidelity of the spectrum depends in this case on several factors, including the relative orientation between prism and FPA; the relative sizes of pixel pitch and sensor point spread function; and algorithms to determine spectral calibration and content. In this paper, we elucidate some methods for extracting the spectral data from the two-dimensional array of measurements, including the use of radial basis functions, and demonstrate the procedure with data from a spectral imager.

Keywords: spectrometer, dispersion, spectrum, radial basis functions

1. INTRODUCTION

Spectral imaging has become an important analysis tool for a wide range of applications. Spectral imaging has been used in remote sensing to perform geological surveys, trace the origins of pollution, locate mineral deposits, assess agricultural productivity, and characterize effluents. At present, the military is interested in spectral imaging for characterizing littoral environments, locating tanks under trees, and discovering the location of buried mines. Recently, spectral imaging has also found limited application in medical imaging¹ and the development of herbicides^{2,3}, among other things.

Spectral imaging is the art of quantifying the spectral and spatial characteristics of a scene. A spectral image usually consists of a sequence of monochromatic images, where each monochromatic image represents the scene as it would appear when viewed over a limited wavelength band, and each image in the sequence is centered at a unique wavelength. Spectral images are inherently three-dimensional: two spatial components and one chromatic component, which together form the so-called spectral data cube as seen in Fig. 1. The collection of brightness values from the same pixel location in each of the monochromatic images forms the optical spectrum of the reflected and/or radiated energy from the corresponding object location. In this sense, a spectral imager can be considered a spectrometer for an array of barely-resolved image elements, where each image element is the size of a pixel. Thus, unlike a traditional non-imaging spectrometer, spectral imagers capture the spectral content of points over a potentially wide field of view (FOV).

On its basic level, a typical spectral imaging system uses a dispersing element, such as a prism or a diffraction grating, in front of an imaging camera: the dispersing element provides color separation on the camera's focal plane array (FPA). Since the FPA is inherently two-dimensional, some type of multiplexing is required to acquire the spectral data from the scene. In scanned slit instruments like pushbroom and whiskbroom sensors, one spatial and one spectral dimension are measured on the FPA at each camera frame, and the remaining spatial dimension is scanned in time. Other multiplexing methods can also be employed, such as tomographic systems^{4,5} that measure a sequence of different projections through the spectral data cube in order to mathematically reconstruct it; however, the basic components of these systems remain a dispersing element and an imaging camera. Furthermore, the temporal multiplexing process introduces artifacts when

* rick@solidstatescientific.com; phone (603) 598-1194; fax (603) 598-1197.

the scene is not static. Therefore, most spectral imagers work well for static objects, but fail to accurately represent the scene when platform motion or scene evolution is present. Typically, restricting the spatial resolution so that intra-scene motion is contained within a pixel mitigates the effect of scene motion; nevertheless, the effects of platform motion are sometimes evident.

While the vast majority of the effort in spectral imaging to date has focused on static scenes, dynamic spectral imaging is now attracting attention. Simultaneous spectral imaging can provide useful data for rapidly evolving scenes and change detection. Algorithms based on spectral-temporal image data can be used to classify energetic events such as plumes, explosions, and biomass fires. The temporal evolution of the event signature can also provide information about the changing constituents of energetic events, such as the identity and timing of primary and secondary explosions. In particular, it is often the spectral content of an energetic, unresolved point target, rather than a resolved image, that becomes the subject of measurement or study. Since many of these point targets are “un-cued” (unannounced in either location, time, or both), methods for using potentially wide FOV spectral imagers as point target spectral-temporal sensors can be particularly attractive.

Spectral imaging systems that use a dispersive element to disperse the colors onto the focal plane can serve as a spectrometer for point events in a non-imaging mode. The resulting spectral or spectral-temporal sensor can readily measure the point target’s spectrum with minimal computational load because the spectral data from a point event is spread directly on the FPA. In what follows we elucidate some methods for extracting the spectral data from the two-dimensional array of measurements, including the use of radial basis functions, and demonstrate the procedure with data from a spectral imager.

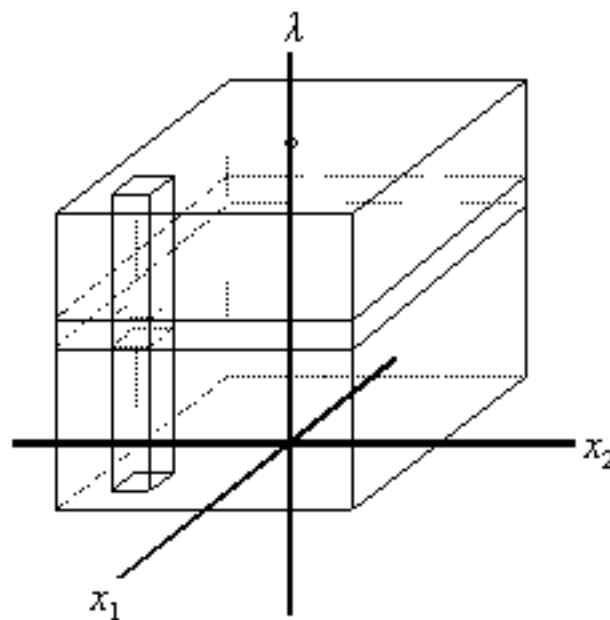


Figure 1. The Spectral Data Cube. The x_1 and x_2 axes represent the two spatial dimensions of the image, and data values parallel to this plane represent the image of the scene for a narrow wavelength band. The column in the figure represents the spectral values (spectrum) from an object pixel location.

2. IMAGER AS SPECTROMETER

As noted above, a typical spectral imaging system uses a dispersing element in front of an imaging camera, such as the arrangement shown in Fig. 2. In this rendering, the dispersing element is a direct vision prism, which allows one wavelength of light—called the “un-deviated” wavelength—to pass without deviation, while all other wavelengths are deviated from the optical axis. The amount of angular deviation is a function of the difference between the un-deviated wavelength and the wavelength in question. A broadband point source will be spread by the direct vision prism into a line spectrum that is focused on the FPA of the camera. This setup will be the model for the following analysis, although the identification of a direct vision prism as the dispersing element is not important: a standard wedge prism or even a diffraction grating could be substituted with similar results.

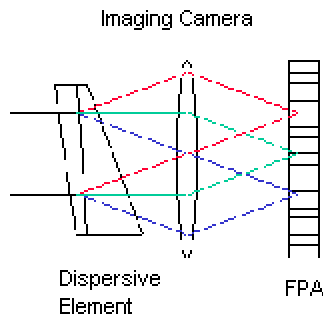


Figure 2. Basic Spectral Imager. At its basic level, a spectral imager is a dispersive element, such as a prism or grating, placed in front of a digital camera. When operating in a non-imaging mode, the spectrum from a point source is spread along a line on the FPA.

If the aperture for the system allows the full FOV of the system to be focused on the FPA (i.e., not a slit imager), each object point will form a spectrum on the FPA. In general, the spectra from neighboring object points will overlap on the FPA. For purposes of the following development, we assume that the object of study is an energetic, unresolved source in an otherwise cool and known background. This is not unrealistic: it is possible to measure the background prior to the onset of the energetic event. The background frame is then subtracted from the frame containing the desired point target, resulting in a “background-corrected” data frame. Fig. 3 shows an example.

Ideally, the corrected data frame contains only the spectral signature values from the point source, sampled on the FPA; in reality, the data frame contains the difference in spectral signature values between the desired target and that portion of the background obscured by the target, as well as noise from background drift and from the sensor itself. Often the difference in spectral signature between target and obscured background is small for energetic targets for two reasons: the effective temperature difference between target and background is large, and, if the emitting area of the unresolved target is much smaller than an object pixel, the target approaches a true point, making the difference inconsequential. In addition, if the background frame is measured immediately before the onset of the event (and its measurement), noise due to background drift is minimized; consequently, sensor noise is typically the largest noise component.

It remains to extract the spectrum from the corrected data frame. Since the spectral resolution is limited by the smallest sampling interval, we expect the extracted spectrum to be the brightness values of the point source spectrum as if sampled at a discrete set of wavelengths whose corresponding geometric rays would each land on the FPA with a spacing equal to the pixel pitch. Thus, one way to interpret the extracted spectrum is as a series of continuous narrow

wavelength bands (or colors), with each band centered at the wavelengths that correspond to pixel centers and the width of each band corresponding to the width of a pixel.

In order to account for the signal on the focal plane, the spectral extraction process must incorporate the measured brightness values at each pixel location. The process is equivalent to assigning, for the brightness value measured at each pixel, what portion of the brightness value belongs in each spectral band. This is not a trivial process, since the point source is spread by the point spread function of the sensor in two dimensions, and the sampling represents a convolution of the point spread function with the source, integrated over each pixel's active area. A simple estimate of the spectral shape might be made by orienting the dispersive element so as to disperse the spectral energy from the point source along a horizontal line on the FPA, and then simply sum the pixel columns. This process, however, neglects several important points:

1. The spectrum cannot be calibrated without knowledge of a spectral feature. . Because the spectral energy is spread along a line, even if the dispersion characteristics of the sensor are known it is impossible to assign a wavelength value to each pixel location without a reference. Although it is possible to estimate the location of an object in one dimension only from the spectral line, this dimension cannot calibrate the spectrum with wavelength. Calibration can be performed by correlating the object location (i.e., the centroid of the point source as imaged without a dispersive element) with a particular wavelength of light,

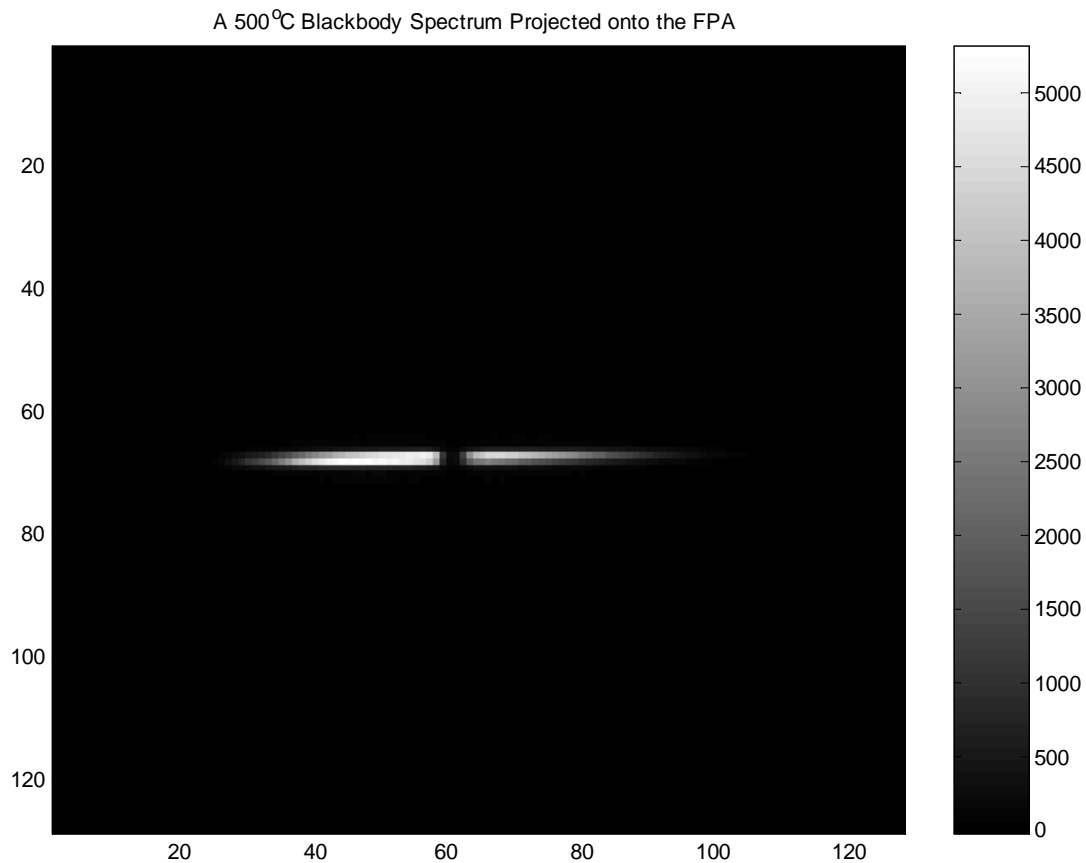


Figure 3. A "Background Corrected" Data Frame. The 128x128 image shows the measured ADU levels in each pixel, after subtraction of a background frame. The point target is a small-aperture 500°C blackbody source located 100 ft from the sensor.

or by some other means. For the purposes of this development, it will be assumed that the location of the point source image on the FPA is known, and that the wavelength of light is known to which this position corresponds when the dispersive element is inserted.

2. Spectral energy is spread by the point spread function of the sensor, perpendicular to the spectral line. Although the column sum attempts to account for this spread, the integral number of pixel rows over which to perform the sum may artificially truncate the signal unevenly (and include noise unevenly) if the image of the source is not located at the vertical center of a pixel row. Increasing the number of rows over which to perform the sum may mitigate this problem, but doing so adds corrupting sensor noise.
3. Spectral energy is spread by the point spread function of the sensor along the spectral line. The brightness values measured at the sampled pixels represent a convolution over the entire band pass of the sensor, and in particular, incorporate a continuum of wavelengths that do not yield to the hard boundaries imposed by the pixel columns.
4. Misalignment between dispersive element and FPA pixel rows can create spectral artifacts. This problem can be partially mitigated by estimating the alignment directly from the sampled data using a least-squares line fit, with the measured brightness values at the pixel locations serving as the weights in the cost function. However, if the spectral line is horizontal but not vertically centered on a pixel row, a systematic error in the line location will result. Consequently, a least-squares fit is more accurate when the dispersive element is tipped relative to the FPA, effectively randomizing the phase of the systematic errors.

To address these concerns, a technique using radial basis functions to extract the spectral content from the 2-dimensional FPA has been developed based on the use of radial basis functions.

3. DETERMINATION OF SPECTRUM

In recent years, radial basis function approximations to non-linear functions have proven indispensable in automatic control theory, especially in establishing neural networks as a popular alternative to the relatively slowly-converging multilayer perceptron models⁶. For our purposes, a radial basis function (RBF) is defined as follows⁷:

Definition 1. A Radial Basis Function is a real mapping $\phi_{\chi, \sigma} : \mathfrak{R}^n \rightarrow \mathfrak{R}$ with center $\mathbf{c} \in \mathfrak{R}^n$, scaling constant $\sigma \in \mathfrak{R}_+$, and where ϕ is constant on spheres $\{\mathbf{x} \in \mathfrak{R}^n \mid \|\mathbf{x} - \mathbf{c}\| / \sigma = r\}$ at radius $r\sigma$, $r \in \mathfrak{R}_+$. (Usually the Euclidian norm on \mathfrak{R}^n is used as the definition of $\|\cdot\|$.)

Kolmogorov's representation theorem guarantees that any function continuous on the n -dimensional unit cube E^n can be represented by a suitably-weighted linear combination of RBFs, and that the functional form of the RBFs are independent of the function to be estimated⁸. Consequently, the scalar output $f(\mathbf{x})$ of a single-layer RBF network is usually written as a linear combination of weighted RBFs:

$$f(\mathbf{x}) = w_0 + \sum_{i=1}^N w_i \phi_i(\|\mathbf{x} - \mathbf{c}_i\|), \quad (1)$$

where N is the number of RBFs, w_0 is an offset or bias, \mathbf{c}_i is the RBF center (location), and the norm is the Euclidian distance between the current point of interest \mathbf{x} and the center \mathbf{c}_i of RBF ϕ_i .

In automatic control, adaptive networks within the RBF framework are created to estimate the best number of radial basis functions to be used, the center locations for the RBF's, and the constant (σ). Data at the sampled locations are used to "train" the network, i.e., determine the best weights w_i , so that the function $f(\mathbf{x})$ as defined in (1) best fits the sampled data. In this way, the RBF expansion approximates $f(\mathbf{x})$ for any desired \mathbf{x} as an optimized interpolator between sample points^{9,10}.

Conceptually, estimating the spectral content of a point target with radial basis functions works as follows. The center of each pixel on the FPA is considered the sample location for the brightness value associated with it. The dispersion on the FPA due to the point source defines a line on the FPA given by

$$\mathbf{y}_L(\lambda) = \mathbf{y}_0 + \alpha(\lambda - \lambda_0)\mathbf{d}, \quad (2)$$

where \mathbf{y}_L is the point on the line where a ray of light corresponding to wavelength λ would arrive, \mathbf{y}_0 is the location of a spectral reference (of wavelength λ_0), \mathbf{d} is a unit vector that describes the relative orientation between dispersion direction and the FPA, and $\alpha(\lambda - \lambda_0)$ describes the dispersion of the dispersive element and imaging system. On this line, at discrete locations \mathbf{c}_i , are placed radial basis functions, which, when appropriately weighted, sum to the brightness values at the pixel locations. The estimated value of the spectrum at any wavelength λ can then be obtained by computing the position along the line from Eq. (2), and substituting this location into the interpolating equation (1).

Some possible functional forms for the radial basis functions are shown in Table 1. The value of σ in the radial basis functions in effect scales the size of the RBF, i.e., determines how quickly the function approaches zero as the distance from its center grows without bound. On a practical note, this scale can be set to correspond to the actual point spread function of the system, if known. Otherwise, it can be estimated from the data itself by determining the spread in brightness value of each pixel as a function of the orthogonal distance from each pixel center to the line in Eq. (2). In this latter case, the best value for σ will be less than the spread in the data when the actual point spread function scale is the size of a pixel or greater.

Table 1. Some RBF Functions for Spectral Extraction.

$\phi(\mathbf{z}) = \exp\left(\frac{-\ \mathbf{z}\ ^2}{2\sigma^2}\right)$	Gaussian
$\phi(\mathbf{z}) = \frac{1}{\sqrt{\ \mathbf{z}\ ^2 + \sigma^2}}$	Inverse Multiquadratic
$\phi(\mathbf{z}) = \left[\frac{J_1(\ \mathbf{z}\ /\sigma)}{(\ \mathbf{z}\ /\sigma)} \right]^2$	Airy

The n -dimensional sampling theorem provides that if the continuous spectrum, as spread on the FPA, has a vanishing Fourier transform outside a bounded subset of n -dimensional space, then the spectrum can be exactly reconstructed from its samples at appropriately-placed lattice points (to ensure no aliasing)¹¹. Although there is no guarantee that the 2-D function sampled on the FPA satisfies the Nyquist criterion, it is important to note that the object of the spectral extraction is to determine the certain spectral weights along the line of Eq. (2), and not the point spread function of the spectrometer. Assuming the band pass of the sensor and the noise characteristics allow the measurement of N spectral bands, the RBF expression in Eq. (1) can be simply expressed as:

$$\mathbf{f}_m = \mathbf{P} \mathbf{w}_n, \quad (3)$$

where

$\mathbf{f}_m =$ ($M \times 1$) vector of brightness values associated with pixel centered at location \mathbf{x}_m ;

$\mathbf{P} =$ ($M \times N$) matrix of distance-weighted RBF values where the elements $[\mathbf{P}]_{m,n} = \phi(\|\mathbf{x}_m - \mathbf{y}_0 - n p \mathbf{d}\|)$, where p is the pixel pitch on the FPA and $(K - N) < n \leq K$ for some integer K ;

$\mathbf{w}_n =$ ($N \times 1$) vector of RBF weights.

Note that the subtraction of the background frame should, in theory, eliminate the bias term w_0 , and that K depends on the characteristics of the dispersive element. The RBFs are placed along the spectral line with spacing equivalent to the

pixel pitch, and use the spectral reference for calibration. Importantly, with this placement of RBFs, the weight vector \mathbf{w}_n is the desired spectrum. If the RBF is normalized with respect to its integrated area, the spectrum will be expressed in measurement units¹² (usually ADUs).

Typically $M \gg N$, and determination of the spectrum \mathbf{w}_n is reduced to a problem in linear algebra:

$$\mathbf{w}_n = (\mathbf{P}^T \mathbf{P})^{-1} \mathbf{P}^T \mathbf{f}_m. \quad (4)$$

In implementing Eq. (4), care should be taken to ensure the condition number of the matrix $\mathbf{P}^T \mathbf{P}$ will allow for successful inversion; otherwise, the data may allow a solution only for smaller N .

4. EXAMPLES

Shown below are the spectral extractions using the RBF technique on two different point sources. The sensor used to measure the data is the MWIR CTHIS instrument, developed as a tomographic spectral imager. The optical system consists of a telescope, direct vision prism, and imaging camera. Normal operation of the camera as an imager involves recording at several different prism orientations the spread of light, as dispersed by the direct vision prism, from a static scene. Normally the several frames are then used to mathematically reconstruct the spectral image. When operated in non-imaging mode for point targets, as in the figures below, only two frames of data need be collected: one of the background without point source, and one of the background with the point source. For this imaging sensor, the dispersive element provides about 74 spectral bands between about 2.8 μm and 5.5 μm .

Fig. 4 shows the image of the same 500°C blackbody source as depicted in Fig. 3, except the dispersive element has been tipped relative to the FPA. The point target is a small-aperture located 100 ft from the sensor. The corresponding spectral extraction, using the RBF technique, is depicted in Fig. 5. Note that the exitance from this point source is a smooth Planck curve, with a maximum at 3.74 μm ; however, the irradiant spectrum at the focal plane is an attenuation of the exitance by the optical transmission of the atmosphere (including the atmospheric absorption near 4.3 μm due to CO_2) and optics.

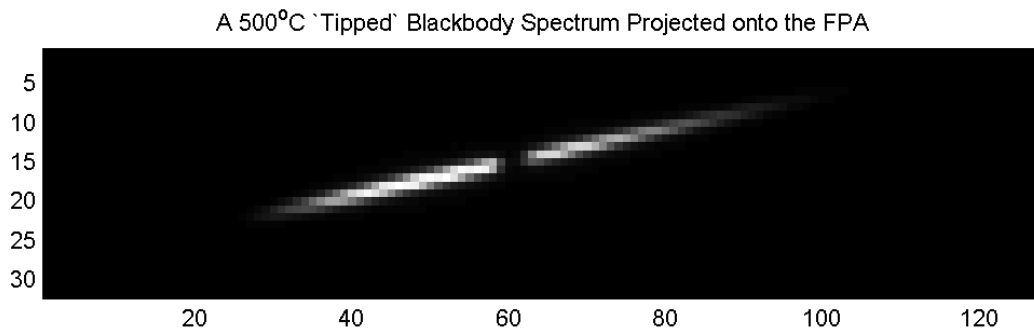


Figure 4. A "Background Corrected" Data Frame with Tipped Spectral Line. The 32×128 image shows the measured ADU levels in each pixel, after subtraction of a background frame. The point target is a small-aperture 500°C blackbody source located 100 ft from the sensor, and is the same source shown in Fig. 3, except that the dispersive element is purposely tipped relative to the pixel lattice.

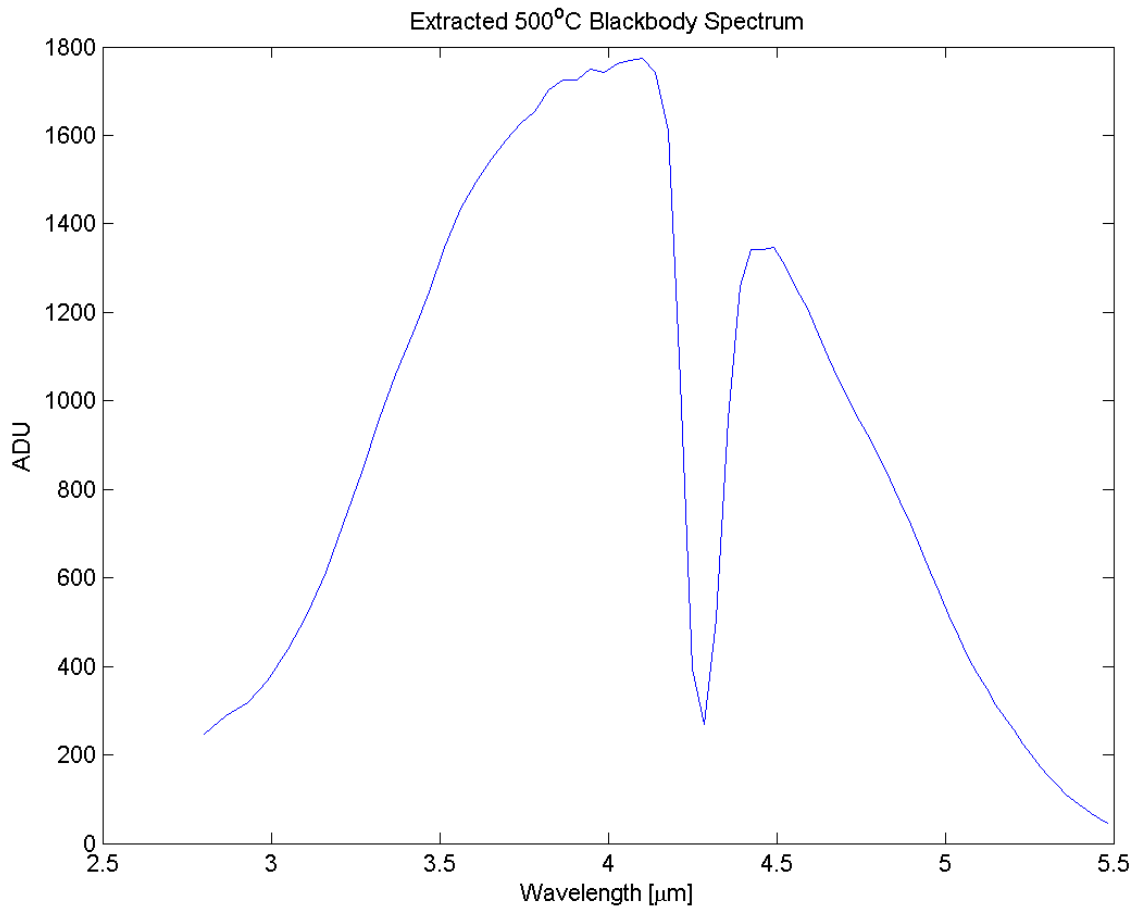


Figure 5. Spectrum from a Blackbody. The point target is a small-aperture 500°C blackbody source located 100 ft from the sensor. This extraction is from the frame of data shown in Fig. 4. Note that the spectral shape is changed from an expected blackbody curve by the optical transmission of the atmosphere and sensor optics.

For comparison, we include the a spectral extraction from a propane torch. The propane source is made a point source by using a small aperture to limit the spatial extent. No comparison should be drawn from the difference in relative intensity values between the propane spectrum and the blackbody spectrum of Fig. 5, since the sources were measured at different distances, different radiating areas, integration times, optical telescopes, and atmospheric conditions. Instead, the spectra are provided as an example of the RBF extraction technique.

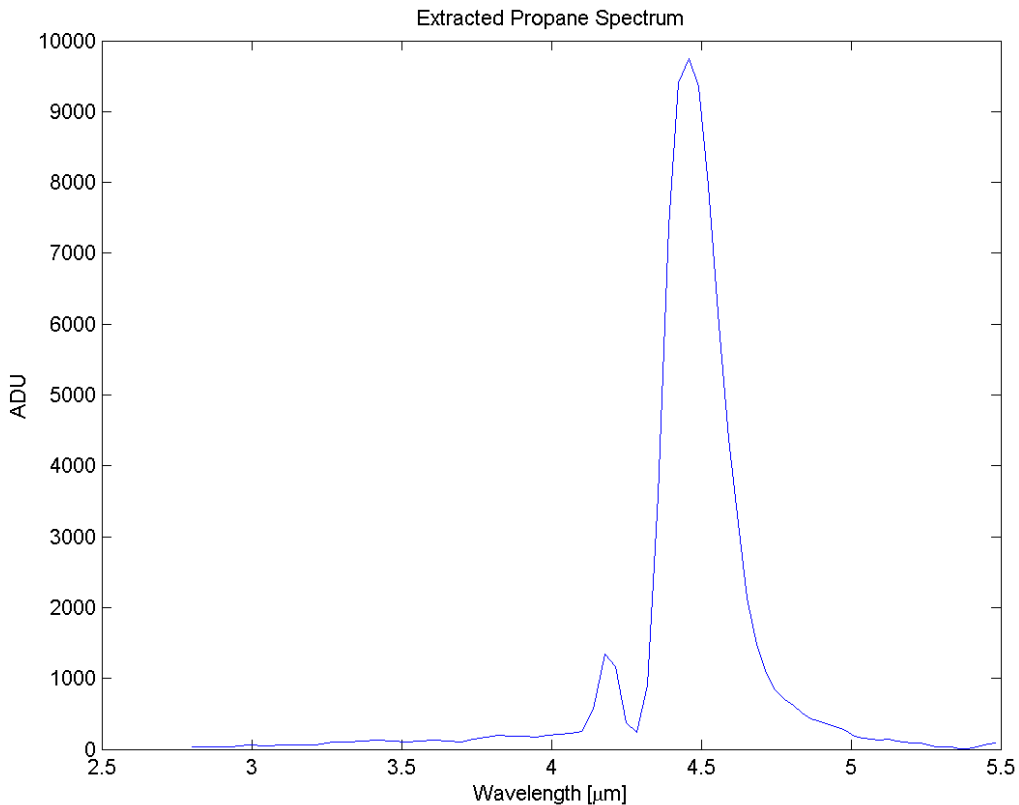


Figure 6. Spectrum from a Propane Torch. The point target is a propane torch located 10 ft from the sensor, as seen through a small aperture.

5. CONCLUSIONS

A spectral imaging system that uses a dispersing element and a camera can be used in a non-imaging mode as a spectrometer for point events with minimal computational load because the spectral data from a point event is spread directly on the FPA, usually along a line. The FPA pixel pitch determines the highest sampling frequency of the continuous spectrum, and the task of extraction becomes one of assigning a portion of the brightness values at each measured pixel location to spectral bands. The task is complicated by the (unknown) point spread function of the sensor, and the (unknown) active area of the pixels. In addition, sensor noise errors in the spectral extraction can be minimized by tipping the dispersion direction relative to the pixel lattice, effectively randomizing the bands to which sensor noise is assigned, but doing so further complicates the spectral extraction task. The spectrum can nevertheless be deduced by estimating the 2-dimensional brightness values, assumed measured at the pixel centers, as a linear combination of radial basis functions placed along the spectral line. Finally, future work will establish the fidelity of the spectral extraction when compared with ground truth.

ACKNOWLEDGEMENTS

This work was done under Air Force Contract F19628-01-C-0059. The author also expresses appreciation to Dr. Jon Mooney for many insightful discussions.

REFERENCES

-
- ¹ X.F. Wang and B. Herman, eds. *Fluorescence Imaging Spectroscopy and Microscopy*. Chemical Analysis Series, vol. 137. Wiley & Sons: New York, 1996.
- ² P.J.B. Hancock, R.J. Baddeley, and L.S. Smith. “The Principal Components of Natural Images.” *Network* 7:261–266, 1996.
- ³ A.F.H. Goetz, et. al. “Imaging Spectrometry for Earth Remote Sensing.” *Science*, 228:1147–1153, 1985.
- ⁴ J.M. Mooney. “Angularly Multiplexed Spectral Imager.” *SPIE Proc.*, 2480:37–47, 1995.
- ⁵ M.R. Descour, C.E. Volin, E.L. Dereniak, K.J. Thome, A.V. Schumacher, D.W. Wilson, and P.D. Maker. “Demonstration of a High-speed Nonscanning Imaging.” *Opt. Lett.* 22:16, 1997.
- ⁶ K. Warwick, C. Kambhampati, P. Parks, and J. Mason. “Dynamic systems in Neural Networks.” In K. J. Hunt, G.R. Irwin, and K. Warwick, eds. *Neural Network Engineering In Dynamic Control Systems*. Springer-Verlag: London, 1995.
- ⁷ R. Zbikowski and A. Dzielinski. “Neural Approximation: A Control Perspective.” In K. J. Hunt, G.R. Irwin, and K. Warwick, eds. *Neural Network Engineering In Dynamic Control Systems*. Springer-Verlag: London, 1995.
- ⁸ A. N. Kolmogorov. “On the Representation of Continuous Functions of Several Variables by Superpositions of Continuous Functions of a Smaller Number of Variables.” *Dokl. Akad. Nauk SSSR*, 108:179–182, 1956.
- ⁹ F. Girosi and T. Poggio. “Neural Networks and the Best Approximation Property.” *Biol. Cybernetics*, 63:169–176, 1990.
- ¹⁰ I.W. Sandberg. “Approximation Theorems for Discrete-time Systems.” *IEEE Transactions on Circuits and Systems*, 38:564–566, 1991.
- ¹¹ T. Kaczorek. *Two-Dimensional Linear Systems*. Springer-Verlag: Berlin, 1985.
- ¹² J. Mooney. Private Communication.